Hydration Products in Water Suspension of Portland Cement Containing Carbonates of Various Solubility

Simona Medvešček,[a]* Roman Gabrovšek,[b] Venčeslav Kaučič,[b] Anton Meden[a]

[a] *Faculty of Chemistry and Chemical Technology, University of Ljubljana, Aškerčeva 5, SI-1000 Ljubljana, Slovenia*
[b] *Laboratory for Inorganic Chemistry and Technology, National Institute of Chemistry, Hajdrihova 19, SI-1001 Ljubljana, Slovenia*

Abstract

The development of hydrated phases and overall microstructure were studied in the course of the hydration of portland cement containing carbonates of various solubility. Phase composition of hydrated samples was examined by powder diffraction and thermogravimetric analysis (TG/DTG). The development of hydrated surfaces was assessed by the measurement of surface area.

The addition of a constant amount of slightly soluble ($CaCO_3$, $MgCO_3$), medium soluble (Li_2CO_3) and highly soluble (K_2CO_3 and $KHCO_3$) carbonates significantly influenced both the degree of hydration and final phase composition of hydrated cement. Anhydrous mineral, tilleyite, was formed in samples containing medium- and highly soluble carbonates.

Keywords: Portland cement; hydration; carbonates; solubility; powder diffraction; thermogravimetry.

Introduction

The production and use of Portland cement containing limestone, blended with cement clinker, has increased particularly in the past twenty years due to mainly technical but also to economical and environmental reasons. The technical reasons are appropriate physical and mechanical properties of hydrated cement paste according to valid standard requirements, and the economical as well as environmental reasons include primarily energy savings for less clinker produced and consequently the reduction of environmental pollution by the greenhouse gas (CO_2). European standard EN 197-1 and the corresponding Slovenian one SIST EN 197-1 allow up to 35 wt % of limestone in cement.[1]

The hydration of Portland cement clinker minerals is essentially their reaction with water yielding a variable-composition complex microstructure comprising amorphous or near-amorphous calcium silicate hydrate gel of nonstoichiometric composition with variable CaO/SiO_2 and H_2O/SiO_2 ratios of 1.5-2.0 and 3.0-4.0, respectively (CSH); calcium aluminate hydrate (e. g. hydrogarnet, $3CaO \cdot Al_2O_3 \cdot 6H_2O$); ettringite, AFt phase, $3CaO \cdot Al_2O_3 \cdot 3CaSO_4 \cdot 32H_2O$, (E); calcium monosulfoaluminate, AFm phase, $3CaO \cdot Al_2O_3 \cdot CaSO_4 \cdot 12H_2O$ (monosulfate, MS), calcium hydroxide ($Ca(OH)_2$), carbonated silicate- (e. g. scawtite, $6CaO \cdot 6SiO_2 \cdot CaCO_3 \cdot 2H_2O$), and/or aluminate hydrated phases (e. g. monocarboaluminate, $3CaO \cdot Al_2O_3 \cdot CaCO_3 \cdot 11H_2O$) and calcium carbonate ($CaCO_3$).

The presence of limestone in Portland cement influences the rate and degree of cement hydration as well as and the phase composition of hydrated cement paste.[2,3] The addition of limestone increases the hydration rate of clinker minerals ($3CaO \cdot SiO_2$ and $2CaO \cdot SiO_2$).[4-6] The acceleratory effect is more pronounced with increased content and greater fineness of limestone.[4,7] The formation of ettringite is also enhanced but its tendency to transform to monosulfate is diminished.[4,8] Monosulfate is further converted into a more stable monocarboaluminate; the remaining monosulfate reacts with the liberated SO_4^{2-} anions and ettringite is formed.[9] Calcium silicate hydrate can include CO_3^{2-} anions in its structure and, consequently, calcium silicocarbonate hydrates form.[4,10] Calcium carboaluminate hydrates usually form in cements that are rich in $3CaO \cdot Al_2O_3$.[4,5,8,11]

The aim of the paper is the study of the influence of the solubility of the added carbonates, on the cement hydration products, as measured by TG/DTG and X-ray diffraction. Both methods are well described in the literature.[12-16]

Experimental

Portland cement used was CEM I 52.2 R, Salonit Anhovo, Building Materials, Joint-Stock Co., Anhovo, Slovenia. Table 1 shows chemical and mineralogical analyses of the cement used.

Table 1. Chemical and mineralogical analysis of CEM I 52.2 R.

Chemical analysis		Mineralogical analysis	
CaO:	63.3%	C_3S:	54.9%
SiO_2:	20.6%	C_2S:	17.7%
Al_2O_3:	4.71%	C_3A:	6.6%
Fe_2O_3:	3.50%	C_4AF:	10.7%
SO_3:	3.37%		
MgO:	1.12%		
K_2O:	0.87%		
Na_2O:	0.21%		
LOI:	1.90%		
Insoluble:	0.37%		

*Standard cement chemistry notations: C: CaO; S: SiO_2; A: Al_2O_3; F: Fe_2O_3.
Compressive strength: 36 MPa (2 days), 56.5 MPa (28 days).

The addition of carbonates was 15 wt % per weight of cement in all cases to facilitate comparison (constant amount of hydrating Portland cement).

The following carbonates were used:

Natural, ground calcite, $CaCO_3$, 99.6%, Magnesia 448, Magnesia GmbH, Lüneburg, Germany. Specific surface area of 2.1 m^2/g (micropore area: 0.3 m^2/g).

Natural, ground magnesite, $MgCO_3$, 98.1%, Magnesia 318, Magnesia GmbH, Lüneburg, Germany. Specific surface area of 4.6 m^2/g (micropore area: 1.0 m^2/g).

Lithium carbonate (Li_2CO_3), potassium carbonate (K_2CO_3) and potassium hydrogen carbonate ($KHCO_3$) were laboratory reagents of p. a. quality.

Portland cement and added carbonate were homogenized and deionized water (w/s ratio of 5) was added. Suspensions were homogenized with VibraCell ultrasonic probe (Sonics & Materials, Inc., USA) for 30 seconds, placed in alkali-resistant flasks, capped airtight and hydrated at 60 °C for 3 to 28 days. The hydration in suspension at 60 °C was chosen with an intention of enhancing the solution phase of cement hydration.

Hydrated samples were filtered, washed with acetone and diethyl ether and dried overnight in a forced-air oven at 40 °C.

Portland cement hydrated under the same conditions was used as a reference.

Thermal analyses were run on SDT 2960 Simultaneous DSC-TGA instrument (TA Instruments – Waters LLC, USA) at 10 °/min from 25 to 800 °C in 100 mL/min N_2 flow. All results (in %) in the paper were calculated by integrating corresponding parts of DTG (derivative thermogravimetric) curves and recalculated to correspond to the ignited mass at 800 °C.

Powder diffraction was performed on Siemens D5000 instrument (Siemens, Germany) with Cu Kα radiation from 5 to 65° 2θ with a step of 0.03° and with 5 s/step.

Surface areas were determined by an automatic gas adsorption analyzer (TriStar 3000, Micromeritics Instrument Corp., USA). Standard 5-point BET method, based on N_2 adsorption at 77 K, was used.

Results and Discussion

Thermal analyses

The composition of the hydrated cement paste was quantitatively evaluated by thermogravimetric analysis using the approach describing in the literature.[12,13,17-26]

Portland cement

Thermogravimetric curve of hydrated cement shows the following characteristic mass losses: desorption of moisture and water desorption from mainly amorphous calcium silicate hydrate gel at about 80-110 °C; the dehydration of ettringite at 130-135 °C; the dehydration of microcrystalline and well-crystallized portlandite, $Ca(OH)_2$, at 390 and 450 °C, respectively; the condensation of structural hydroxyl groups from hydrated calcium silicates at 610-630 °C and the decomposition of carbonated phases and calcite, $CaCO_3$, at 670-700 and 750 °C, respectively.
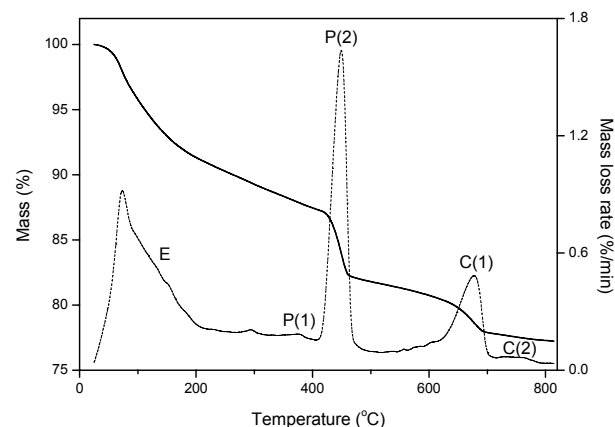
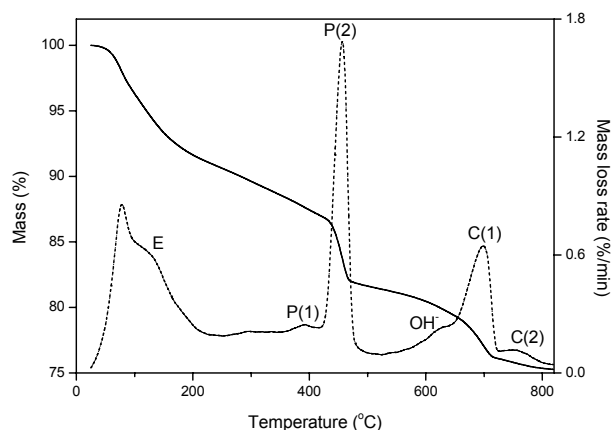

Figure 1. Cement hydrated for 3 days.

Figure 2. Cement hydrated for 28 days.

Figure 3. Cement with $CaCO_3$ hydrated for 3 days.

Figure 4. Cement with $CaCO_3$ hydrated for 28 days.

The comparison between 3- and 28-day hydrated samples, Figures 1 and 2, enables the following conclusions: the content of ettringite (marked E) increases with hydration time; the decomposition temperatures of microcrystalline and crystallized portlandite (marked P(1) and P(2)) shift to higher temperatures with longer hydration time, from 379 to 392 °C for the former and from 449 to 459 °C for the latter. The contribution from structural OH^- groups is clearly visible for 28-day hydrated sample at 620 °C. The peak for amorphous $CaCO_3$ (marked C(1)) also shifts from 676 to 700 °C with prolonged hydration time and increases in area ($CaCO_3$ content from 6 to 8.4%). The peak for well-crystallized calcite (marked C(2)) remains at the same temperature (756 °C), irrespective of hydration time, but calcite content increases.

Surface areas of hydrated products increased from 57 to 66 m^2/g mostly as a consequence of the formation of amorphous and semi-crystalline calcium silicate hydrates with well-developed surfaces. Low values of BET C constant (70-83) indicated no microporosity in analyzed products.

The addition of $CaCO_3$

The effect of calcium carbonate during the hydration of cement is presented in Figures 3 and 4.

The presence of calcium carbonate influences the overall hydration process only to a certain extent. The average content of portlandite was 23.5±0.2%. The increase in both content and decomposition temperature (from 613 to 636 °C for 3- and 28-day hydrated samples, respectively) of structural OH^- groups and amorphous calcite (marked OH- C(1)) can be observed. The content of well-crystallized calcite was equal for both products.

Surface areas of hydrated products increased from 40 to 43.5 m^2/g for 3- and 28-day hydration time,
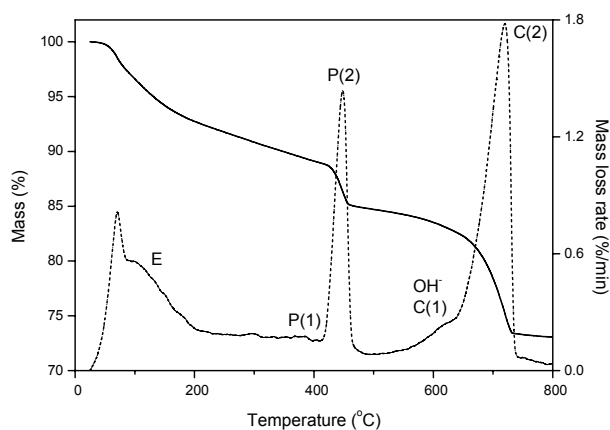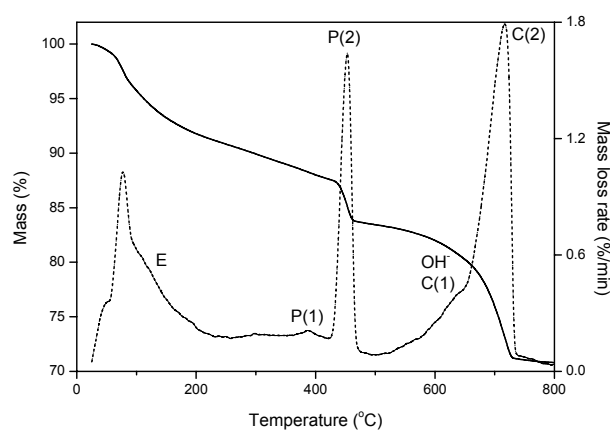
respectively. Measurements indicated that 1.3 and 2.3 m^2/g of surface area originated from micropores (corresponding values of C_{BET} constant: 117 and 136).

The addition of $MgCO_3$

The effect of magnesium carbonate during the hydration of cement is presented in Figures 5 and 6.

The addition of $MgCO_3$ to cement resulted in the formation of brucite, $Mg(OH)_2$, as a consequence of the reaction between $MgCO_3$ and calcium hydroxide. The content of brucite increased with prolonged hydration time. The presence of monosulfate was established in 28-day hydrated product due to its characteristic mass loss at 190 °C (marked MS). An unknown, strong mass loss appeared in 3-day hydrated sample (532 °C, Fig. 5). It also appeared with less pronounced DTG peak at the same temperature in 7-day hydrated sample (not shown here) but it disappeared in 28-day hydrated sample (Fig. 6).

Surface areas of $MgCO_3$-containing products increased from 37 to 47 m^2/g for 3- and 28-day hydration time. There was an indication that 3-day hydration
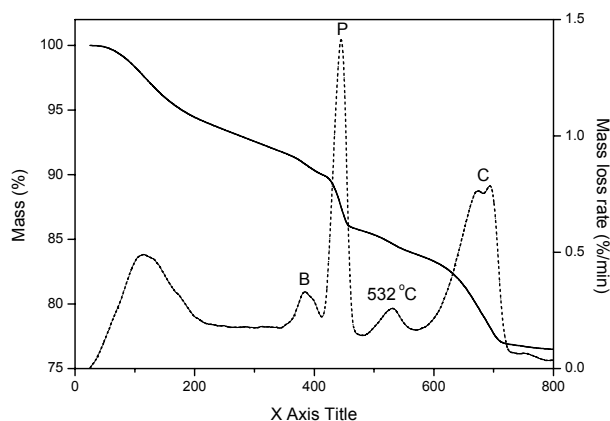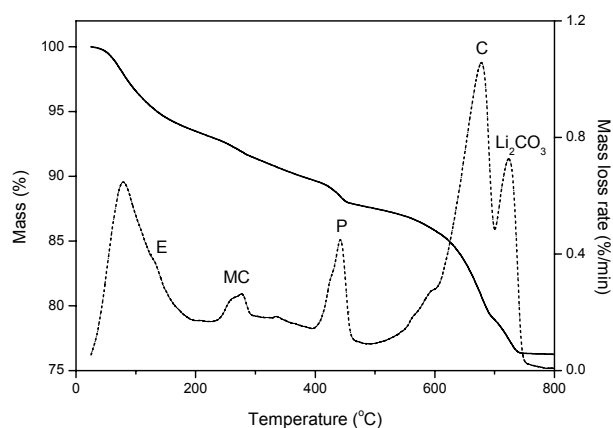
Figure 5. Cement with $MgCO_3$ hydrated for 3 days.

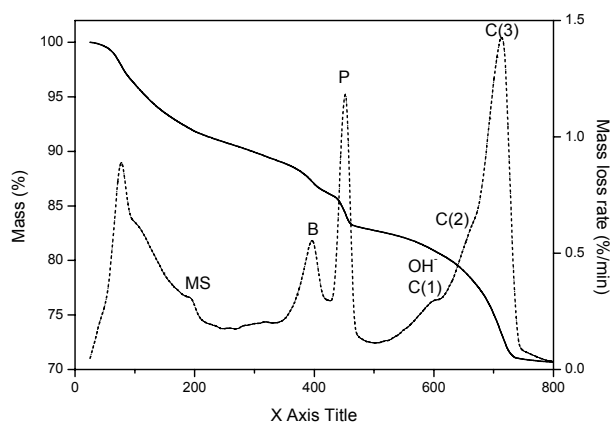**Figure 7**. Cement with Li_2CO_3 hydrated for 3 days.
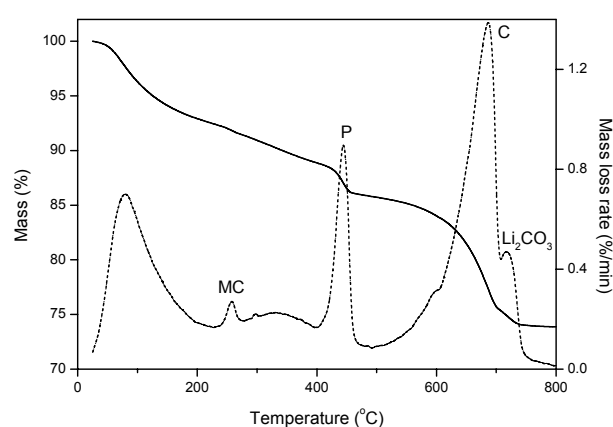

Figure 6. Cement with $MgCO_3$ hydrated for 28 days.

Figure 8. Cement with Li_2CO_3 hydrated for 28 days.

resulted in a product exhibiting 1.5 m²/g of micropore area but after 28-day hydration this effect was no longer apparent.

The addition of Li_2CO_3

The effect of lithium carbonate during the hydration of cement is presented in Figures 7 and 8.

The addition of Li_2CO_3 to cement strongly inhibited its hydration rate within first 3 days of hydration, however, the effect was less pronounced up to 28 days. It was also noticed that total mass loss up to 800 °C decreased after 28-day hydration (18.8%) if compared with corresponding mass loss after 3-day hydration (21.1%). The reason for this behavior was the incomplete hydration of cement and, additionally, the formation of an anhydrous compound, tilleyite, $Ca_5Si_2O_7(CO_3)_2$, the presence of which was confirmed by powder diffraction (ICDD Card 71-2079).

Thermogravimetric curves show the presence of ettringite (marked E) in 3-day hydrated product, but not in 28-day hydrated one. Both samples contain tetracalcium monocarboaluminate (marked MC),

$3CaO·Al_2O_3·CaCO_3·11H_2O$, with a characteristic mass loss between 230 and 250 °C. The content of portlandite is low, what is a consequence of a reaction between Li_2CO_3 and $Ca(OH)_2$ resulting in the formation of LiOH and calcium carbonate (C). The content of the latter increases with longer hydration time. Lithium hydroxide depolymerizes polymeric CSH silicate anions in suspension; the decomposition of these is indicated by a constant mass loss in a broad temperature interval between 300 and 400 °C (Fig. 8). The content of unreacted Li_2CO_3 decreases with prolonged hydration time and it decomposes at 721±3 °C.[27]

Surface areas for Li_2CO_3-containing hydrated products were the lowest of all systems investigated in this study. They increased from 16.5 to 28.5 m²/g for 3- and 28-day hydration time. The same trend for initial micropores presence as decribed above for $MgCO_3$-containing hydrated cement was observed.

The addition of K_2CO_3 or $KHCO_3$

Figures 9 and 10 show the effects of K_2CO_3 addition on the hydration of cement.

The addition of K_2CO_3 resulted in the formation of monosulfate (MS) that was easily detected by its characteristic mass loss with DTG peak maximum at 290 °C.
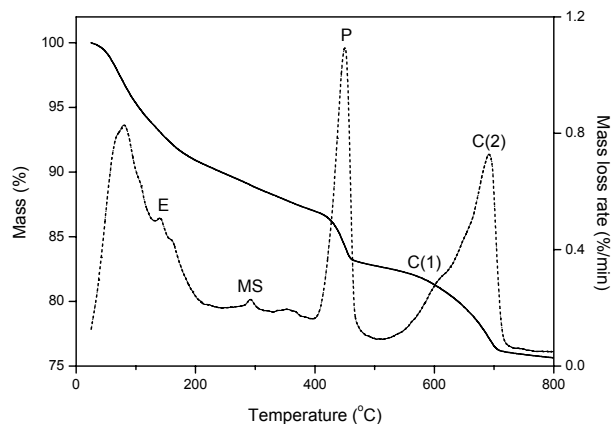

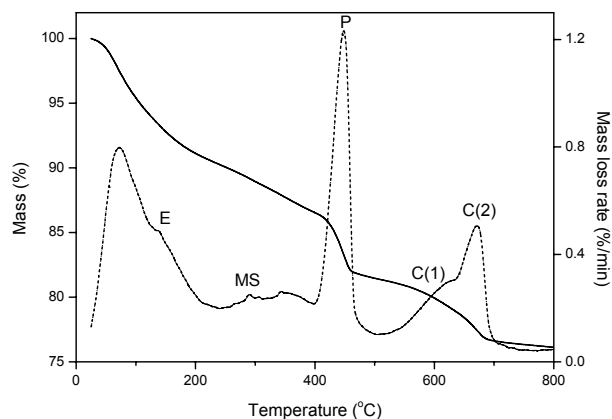**Figure 9**. Cement with K_2CO_3 hydrated for 3 days.

Figure 10. Cement with K_2CO_3 hydrated for 28 days.

The effect of added K_2CO_3 consists of its reaction with gypsum in cement and with the consequent formation of $CaCO_3$ due to its low solubility. Sulfate ions from remaining potassium sulfate react with aluminate part of cement and form ettringite (marked E) which converts into monosulfate (marked MS) with prolonged hydration time. The content of carbonated phases and amorphous $CaCO_3$ (marked C(1) and C(2)) decreases with longer hydration times due to the formation of other carbonate-containing hydrated compounds.

The effect of potassium hydrogen carbonate during the hydration of cement is presented in Figures 11 and 12.

The effect of $KHCO_3$ addition was similar to that of K_2CO_3. The content of monosulfate and amorphous $CaCO_3$ (marked MS and C(2)) was higher in comparison with corresponding hydrated products with added K_2CO_3.
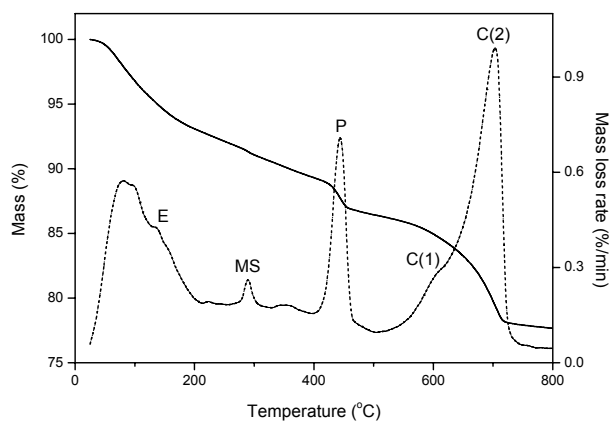

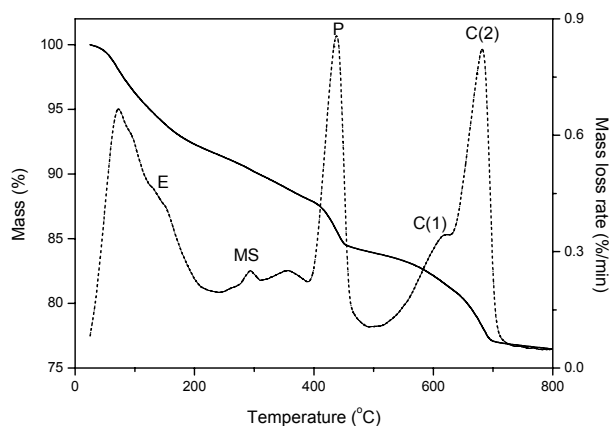**Figure 11**. Cement with $KHCO_3$ hydrated for 3 days.

Figure 12. Cement with $KHCO_3$ hydrated for 28 days.

It can be concluded that lower solubility and lower pH of $KHCO_3$ are the main reasons for similar phase composition, although with different contents of each phase, of hydrated products if compared with results from K_2CO_3-containing hydrated cement.

Portland cement with K_2CO_3 and $KHCO_3$ resulted in the surface area of 31.5 and 32.0 m^2/g, respectively, after the 3-day hydration, but after 28 days the influence of $KHCO_3$ was much higher, resulting in 53.5 m^2/g due to the presence of greater CSH content.

Quantitative results calculated from TG curves are shown in Table 2.

Powder diffraction

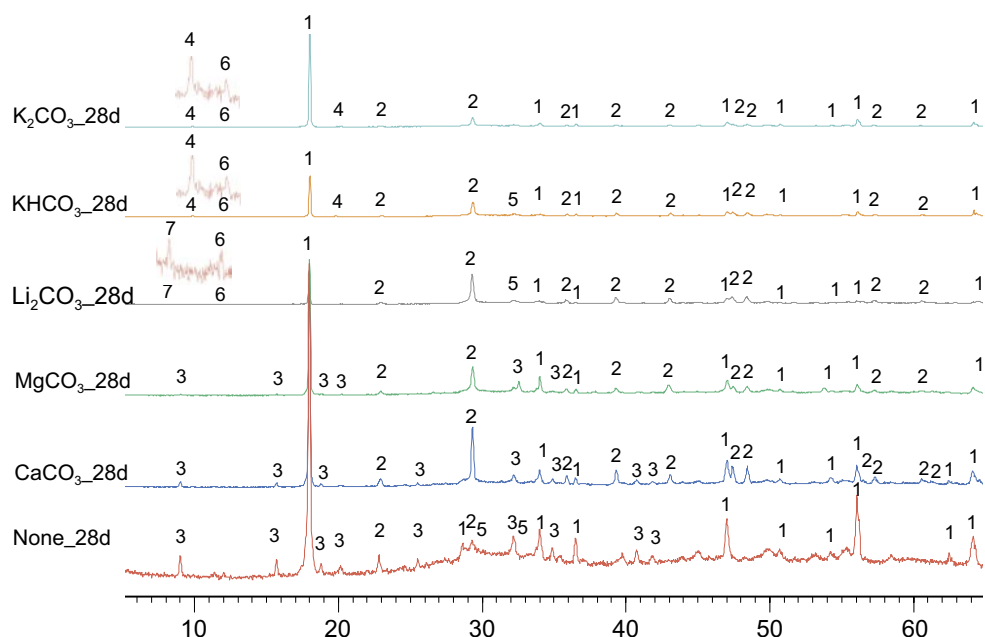Table 3 shows all identified phases during qualitative phase analyses.

The content of particular phase in different samples was estimated on the peak heights.

Table 2. Total mass losses and contents of individual phases in hydrated cements with carbonate additions.

Carbonate added	Surface area (m^2/g)	Total mass loss (%)	$Ca(OH)_2$ (%)	$Mg(OH)_2$ (%)	Amorphous + crystalline $CaCO_3$ (%)	DTG peak maxima (amorphous/crystallized $CaCO_3$) (°C)
None_3d	57	23.7	32.7	-	3.4 + 0.2	675 / 745
None_28d	66	24.1	33.8	-	1.7 + 1.2	661 / 746
$CaCO_3$_3d	40	26.9	23.5	-	2.9 + 12.8	602 / 720
$CaCO_3$_28d	43.5	29.2	23.9	-	4.5 + 13.0	629 / 717
$MgCO_3$_3d	37	23.5	23.4	7.6	6.5 + 2.8	674 / 694
$MgCO_3$_28d	47	29.3	18.8	15.0	4.1 + 9.7	659 / 714
Li_2CO_3_3d	16.5	21.1	11.3	-	2.5 + 8.9	678 / 724
Li_2CO_3_28d	28.5	18.8	16.6	-	2.7 + 11.5	686 / 717
$KHCO_3$_3d	31.5	22.3	15.5	-	0 + 8.4	- / 704
$KHCO_3$_28d	31.5	23.5	21.8	-	0 + 5.5	- / 683
K_2CO_3_3d	32	24.4	23.5	-	2.8 + 6.1	644 / 692
K_2CO_3_28d	53.5	23.9	27.9	-	3.3 + 3.2	620 / 672

Table 3. Mineral phases identified in hydrated cements.

Addition	Portlandite	Calcite	E	MS	Alite	Tilleyite	Additional phases
None_3d	√	√	√	√	√	-	-
None_28d	√	√	√	-	√	-	-
$CaCO_3$_3d	√	√	√	√	√	-	-
$CaCO_3$_28d	√	√	√	-	-	-	-
$MgCO_3$_3d	√	√	√	-	-	-	$MgCO_3$
$MgCO_3$_28d	√	√	√	-	-	-	$Mg(OH)_2$, $MgCO_3$
Li_2CO_3_3d	√	√	-	-	√	√	$NaCa_4Al_2O_6(SO_4)_{1.5} \cdot 15H_2O$
Li_2CO_3_28d	√	√	-	-	√	√	$NaCa_4Al_2O_6(SO_4)_{1.5} \cdot 15H_2O$
$KHCO_3$_3d	√	√	-	√	√	√	-
$KHCO_3$_28d	√	√	-	√	√	√	-
K_2CO_3_3d	√	√	-	√	√	-	-
K_2CO_3_28d	√	√	-	√	-	√	-

Figure 13. X-ray diffraction pattern of hydrated cements and phases identified: 1-portlandite; 2-calcite; 3-ettringite; 4-monosulfate; 5-alite; 6-tilleyite; 7- $NaCa_4Al_2O_6(SO_4)_{1.5} \cdot 15H_2O$; 8-brucite; 9-magnesite.

Portland cement

Powder diffraction enabled the determination of the following phases in hydrated products: tricalcium silicate, $3CaO \cdot SiO_2$, portlandite, $Ca(OH)_2$, calcite, $CaCO_3$, ettringite, $3CaO \cdot Al_2O_3 \cdot 3CaSO_4 \cdot 32H_2O$, and monosulfate, $3CaO \cdot Al_2O_3 \cdot CaSO_4 \cdot 12H_2O$. The presence of calcium silicate hydrate, although established by thermal analysis, could not be identified due to its semi-amorphous nature. Its presence could, however, be concluded from the fact that during the hydration period the content of tricalcium silicate decreased and the content of portlandite increased what altogether indicated the formation of calcium silicate hydrate.[3,29] After 28 days of hydration the content of ettringite increased due to its formation from monosulfate.[29] Carboaluminate phases were not present in any of hydrated samples. The reason for this might be low content of tricalcium aluminate, $3CaO \cdot Al_2O_3$, and the presence of alkalis in cement used.

The addition of $CaCO_3$

X-ray diffraction patterns indicated that the addition of $CaCO_3$ increased the hydration of tricalcium silicate; unreacted tricalcium silicate was present only in 3-day hydrated samples. Portlandite content was comparable to its content in hydrated portland cement regardless of hydration time. Ettringite content increased with hydration time but the content was lower than that in hydrated portland cement. Both contents were, nevertheless, comparable at 28 days of hydration. It seems that carbonate ions slow down the formation of ettringite at the beginning of hydration but as the hydration progresses ettringite formation increases. The presence of monosulfate was established for 3-day hydrated samples but after 28 days monosulfate was no longer detectable. The content of calcite increased with extent of hydration. There was no carboaluminate in any of hydrated samples.

The addition of $MgCO_3$

The content of ettringite, in 3-day hydrated samples, determined by powder diffraction , was lower if compared with $CaCO_3$-containing hydrated samples but after 28 days of hydration both contents were comparable. The presence of brucite, $Mg(OH)_2$ was also confirmed in 28-day hydrated sample.

The addition of Li_2CO_3

According to powder diffraction data the addition of Li_2CO_3 strongly inhibited the hydration of cement: after 3 days of hydration a significant part of tricalcium silicate remained in the product, the content of portlandite was low and there was no ettringite present. The content of tricalcium silicate decreased after 28 days and was comparable to the one in hydrated portland cement. The contents of portlandite and calcite increased from 3- to 28 days of hydration. An anhydrous mineral, calcium silicate carbonate, tilleyite, $Ca_5Si_2O_7(CO_3)_3$ was identified in 3- and 28-day hydrated samples. Additionally, the presence of crystalline phase, sodium calcium aluminum sulfate hydrate, $NaCa_4Al_2O_6(SO_4)_{1.5} \cdot 15H_2O$ was confirmed by its strong reflection at 8.8° 2θ.

The addition of K_2CO_3 or $KHCO_3$

Hydrated cements with added K_2CO_3 or $KHCO_3$ were rather similar. There was some tricalcium silicate after 3-day hydration, after 28 days of hydration unreacted tricalcium silicate appeared only in $KHCO_3$-containing hydrated cement. The content of portlandite increased with the extent of hydration but the content was lower than either in hydrated portland cement or in hydrated cements containing $CaCO_3$, $MgCO_3$ or Li_2CO_3. The same conclusion was found for the content of calcite. All hydrated samples contained monosulfate the content of which was higher in $KHCO_3$-containing samples. The content of monosulfate decreased with the extent of hydration. The presence of tilleyite was also confirmed in all hydrated samples.

Conclusions

We can conclude that the addition of various carbonates significantly influences the whole hydration process and consequently the hydration phases formed. The main effect on the hydration process of portland cement is related to the solubility of carbonate added as the differences become more significant when the solubility increases.

Medium soluble (Li_2CO_3) and highly soluble (K_2CO_3) carbonates inhibit the hydration of tricalcium silicate at the beginning but with prolonged hydration time they obviously act as accelerators (no remaining tricalcium silicate in hydrated samples).

The content of calcite increases with longer hydration times for hydrated products containing slightly-($CaCO_3$, $MgCO_3$) and medium soluble (Li_2CO_3) carbonates but decreases for samples containing highly soluble carbonates (K_2CO_3, $KHCO_3$).

The presence of monocarbonate was not established in any hydrated product up to 28 days of hydration. The reasons for this may be the presence of alkalis in cement, low content of tricalcium aluminate (7-8%), the temperature of hydration or, most likely, the combination of all these factors. The formation

of calcium carboaluminate hydroxides and calcium carboaluminates has thus not taken place to any significant extent within the investigated systems.

CSH formed during the hydration process in cement containing medium- and highly soluble carbonates (Li_2CO_3, K_2CO_3, $KHCO_3$) reacts with the excess of CO_3^{2-} anions and gives in the final effect tilleyite ($Ca_5Si_2O_7(CO_3)_2$).

The formation of monosulfate was rapid in hydrated cements containing highly soluble carbonates but the effect was opposite in hydrated cements containing slightly- and medium soluble carbonates.

Acknowledgments

References

1. European Committee for Standardization; Cement: Composition, Specifications and Conformity Criteria, Part 1: Common Cements, EN 197-1 (**2000**)

2. Klieger, R. D. Hooton (Eds.): Carbonate Additions to Cement, STP 1064, ASTM, Philadelphia, 1990, 81 pp.

3. P. Hawkins, P. D. Tennis, R. Detwiler, The Use of Limestone in Portland Cement: A State-of-the-Art Review, EB 227, Portland Cement Association, Skokie, **2003**, 44 pp.

4. V. L. Bonavetti, V. F. Rahhal, E. F. Irassar, *Cem. Concr. Res*. **2001**, *31*, 853–859.

5. S. Catinaud, J. J. Beaudoin, J. Marchand, *Cem. Concr. Res*. **2000**, *30*, 1961–1968.

6. R.L. Sharma, S.P. Pandey, *Cem. Concr. Res*. **1999**, *29*, 1525–1529.

7. V. Rahhal, R. Talero, *Cem. Concr. Res*. **2005**, *35*, 1285–1291.

8. G. Kakali, S. Tsivilis, E. Aggeli, M. Bati, *Cem. Concr. Res*. **2000**, *30*, 1073–1077.

9. V. Kasselouri, Ch. Ftikos, G. Parissakis, *Cem. Concr. Res*. **1983**, *13*, 649–654.

10. J. Pera, S. Husson, B. Guilhot, *Cem. Concr. Comp*. **1999**, *21*, 99–105.

11. M. A. Trezza, A. E. Lavat, *Cem. Concr. Res*. **2001**, *31*, 869–872.

12. V. S. Ramachandran, Applications of Differential Thermal Analysis in Cement Chemistry, Chemical Publishing Company, Inc., New York, **1969**, 307 pp.

13. V. S. Ramachandran, R. M. Paroli, J. J. Beaudoin, A. H. Delgado (Eds.): Handbook of Thermal Analysis of Construction Materials, Noyes Publications, Norwich, **2003**, 680 pp.

14. Guide to Compounds of Interest in Cement and Concrete Research, Spec. Rep. 127, Highway Research Board, Washington, **1972**, 53 pp.

15. P. E. Stutzman, Guide for X-Ray Powder Diffraction Analysis of Portland Cement and Clinker, NISTIR 5755, NIST, Gaithersburg, **1996**, 38 pp.

16. I. C. Madsen, N. V. Y. Scarlett, in: F. H. Chung, D. K. Smith (Eds.): Industrial Applications of X-Ray Diffraction, Marcel Dekker, Inc., New York, **2000**, pp. 415–440.

17. R. C. Mackenzie, in: H. F. W. Taylor (Ed.): The Chemistry of Cements, Vol. 2, Academic Press Inc. Ltd., London, **1964**, pp. 271–288.

18. W. Wm. Wendlandt, Thermal Methods of Analysis, John Wiley & Sons, Inc., New York, **1964**, 424 pp.

19. V. S. Ramachandran, *Thermochim. Acta* **1972**, *4*, 343–366.

20. V. Kasselouri, Ch. Ftikos, G. Parissakis, *Cem. Concr. Res*. **1983**, *13*, 649–654.

21. V. S. Ramachandran, C.-M. Zhang, *Mat. Struct*. **1986**, *19*, 437–444.

22. J. G. Dunn, in: J. D. Winefordner (Ed.): Treatise on Analytical Chemistry, Part 1, Volume 13, 2nd Edition: Thermal Methods, John Wiley & Sons, Inc., New York, **1993**, pp. 127–266.

23. J. J. Garcia-Escalante, J. H. Sharp, *Cem. Concr. Res*. **1998**, *28*, 1245–1257.

24. J. Dweck, P. F. Ferreira Da Silva, P. M. Büchler, F. K. Cartledge, J. Therm. Anal. Calorim. **2002**, *69*, 179–186.

25. R. Vedalakshmi, A. S. Raj, S. Srinivasan, K. G. Babu, *Thermochim.* Acta **2004**, *407*, 49–60.

26. I. Pane, W. Hansen, *Cem. Concr. Res*. **2005**, *35*, 1155–1164.

27. J.-W. Kim, Y.-D. Lee, H.-G. Lee, *ISIJ Int*. **2004**, *44*, 334–341.

28. P. K. Mehta, P. J. M. Monteiro, Concrete: Microstructure, Properties and Materials, 2nd Ed., University of California, Berkeley, **2001**, 239 pp.

29. C. J. Warren, E. J. Reardon, *Cem. Concr. Res*. **1994**, *24*, 1515–1524.

Povzetek

Razvoj produktov in celotne mikrostrukture smo preučevali na hidratiziranih vzorcih portland cementa, ki je vseboval različno topne karbonate. Fazno sestavo hidratiziranih vzorcev smo določali s pomočjo praškovne difrakcije in termogravimetrične analize (TG/DTG), razvoj površine pa ocenjevali z meritvami specifičnih površin.

Dodatek konstantne količine slabo topnih ($CaCO_3$, $MgCO_3$), srednje topnih (Li_2CO_3) in dobro topnih (K_2CO_3, $KHCO_3$) karbonatov očitno vpliva tako na stopnjo hidratacije kot tudi končno fazno sestavo hidratiziranega cementa. Brezvodni mineral, tilejit, se izoblikuje v vzorcih, ki vsebujejo srednje in dobro topne karbonate.